Research Journal of Applied Sciences, Engineering and Technology 11(11): 1245-1256, 2015
DOI: 10.19026/rjaset.11. 2232
ISSN: 2040-7459; e-ISSN: 2040-7467

Submitted: July 24, 2015 Accepted: August 30, 2015 Published: December 15, 2015

Research Article

A Model for a Thin Magnetostrictive Actuator in Nonlinear Dynamics

[1]G.B. Nkamgang, [1]E. Foadieng, [2]V. Kamdoum Tamba, [1]P.K. Talla and [1]A. Fomethe
[1]Laboratoire de Mécanique et de Modélisation des Systèmes Physiques (L2MSP), Dschang, Cameroon
[2]Laboratoire d'Electronique et de Traitement du Signal (LETS), Cameroun

Abstract: In this study, we propose a model for the dynamics of magnetostrictive hysteresis in a thin rod actuator when mechanically the material works in his nonlinear domain. We derive two equations that represent magnetic and mechanical dynamics equilibrium. Our model results from an application of the energy balance principle. The numerical simulations of the model with sinusoidal periodic external fieldgenerate the hysteresis curve and show the equivalent mechanic model. By using the method of multiple scales we analyze the effects of the nonlinear parameter in the system response of magnetostrictive materials. With Routh-Hurwitz theorem, the stability and bifurcation analysis are carried out. Analytical and numerical methods are used to investigate the dynamics of the materials.

Keywords: Actuator, hysteresis, magnetostriction, material, nonlinear

INTRODUCTION

Magnetostriction is the phenomenon of strong coupling between magnetic properties and mechanical properties of some ferromagnetic materials: displacements are generated in response to an applied magnetic field, while conversely, mechanical stresses in the materials produce measurable changes in magnetization. This phenomenon can be used for actuation and sensing. Figure 1 shows a schematic of a Terfenol-D actuator manufactured by Etrema Products Inc. The magnetic field generated by the coil current controls the strain in the Terfenol-D rod, which translates into displacement or force (if blocked) output of the actuator. Like other smart materials (e.g., piezoelectrics and shape memory alloys), such materials exhibit complex nonlinear and hysteretic responses. Modeling and control of their behavior is a challenge. We are interested in obtaining low dimensional models for magnetostriction actuators that show a constitutive coupling in their elastic and magnetic behaviors.

Eddy current losses and magnetoelastic dynamics of the magnetostrictive rod were considered to be the origin of the rate-dependent hysteresis in Vankataraman and Manservisi (2006), Venkataraman and Krishnaprasad (1999, 2005) and Venkataraman *et al*. (1998), where the eddy current losses were modeled by placing a resist or in parallel with a hysteretic inductor and the magneto elastic dynamics was modeled by a second order linear system. Considering a low-dimensional ferromagnetic hysteresis model led to an overall model for magnetostrictive actuators described by a set of switching ordinary differential equations (Venkataraman *et al*., 1998). Tan and Baras (2002, 2004) the authors suggested using a cascade of a Preisach operator with a linear system to model magnetostrictive actuators.

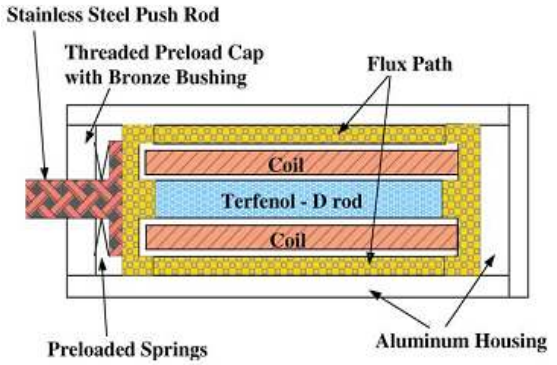

Fig. 1: Sectional view of a *Terfenol-D* actuator manufactured by *Etrema*

However, these previous authors have not taken into account the nonlinear aspect of the displacement in their modeling process. In practical situation the nonlinear terms exist in the displacement and can affect considerably the real dynamics of the material. Thus, our aim in this study is to derive a nonlinear equation for the displacement and use the methods of dynamical systems (lyapunov exponent, bifurcation diagram, Poincare section, spectral diagram), to study the obtained equation.

Corresponding Author: P.K. Talla, Laboratoire de Mécanique et de Modélisation des Systèmes Physiques (L2MSP), Dschang, Cameroon

MATERIALS AND METHODS

According to energy balance principle, the work done by external source (both magnetic and mechanic) is transformed in the change in the free energy of the rod, change in kinetic and losses in the magnetizationprocess and mechanical deformation. This energy balance principe is given by the following equation:

$$\delta W_{bat} + \delta W_{mech} = \underbrace{\delta W_{mag} + \delta W_{magel} + \delta W_{el}}_{change\ in\ internal\ energy} + \underbrace{\delta L_{mag} + \delta L_{el}}_{loss} + \underbrace{\delta E_C}_{change\ in\ kinetic\ energy} \quad (1)$$

In Eq. (1) δW_{bat} is work done by the battery, δW_{mech} is work done by the external force, δE_C is the work done in changing the kinetic energy of the system consisting of the magnetoelastic rod, δW_{mag} is the change in the magnetic potential energy, δW_{magel} is the change in the magnetoelastic energy, δW_{el} is the change in the elastic energy, δL_{mag} are the losses due to the change in the magnetization and δL_{el} are the losses due to the elastic deformation of the rod.

The deformation elastic energy is given by (Pérignon, 2004):

$$\delta W_{el} = \int F(u)du, \quad (2)$$

where, u is the displacement in the rod and F the corresponding force. In the case of large displacement, the corresponding force takes the polynomial form (Chengying and Jin, 2010). When one restricts the development to the cubic order term, the corresponding force becomes:

$$F(u) = k_1 u + k_3 u^3, \quad (3)$$

where, k_1 is the elasticity linear coefficient and k_3 the cubic coefficient. The elastic energychange in one cycle of magnetization is given by (Venkataraman *et al*., 1998):

$$\delta W_{el} = \oint \left(k_1 u + k_3 u^3\right) du. \quad (4)$$

The magnetoelastic energy writes (Venkataraman *et al*., 1998; Krzysztof and Szczyglowski, 2007; Wang and Zhou, 2010):

$$W_{magel} = \nu b M^2 u, \quad (5)$$

where, b is the magneto-elastic coupling constant, ν the volume of magnetostrictive rod and M the average magnetic moment of the rod. The magneto-elastic energy change in one cycle of magnetization is given by:

$$\delta W_{magel} = \oint b \nu M^2 du + \oint 2 b \nu M u dM. \quad (6)$$

According to Jiles and Atherton postulate (Venkataraman *et al*., 1998; Xiaojing and Le, 2007; Jiaju *et al*., 2007), the losses due to hysteresis in one cycle is:

$$\delta L_{mag} = \oint \nu k\, sign(\dot{H})(1-c)dM_{irr}, \quad (7)$$

where,
k = A non-negative parameter
c = Reversibility coefficient
M_{irr} = Irreversible magnetization

The losses due to mechanical damping are assumed to be (Venkataraman *et al*., 1998; Chengying and Jin, 2010; Jiaju *et al*., 2007):

$$\delta L_{el} = \oint c_l \dot{u} du, \quad (8)$$

where, c_l is the damping co efficient.

The change in the kinetic energy is given by (Venkataraman *et al*., 1998; Jiaju *et al*., 2007):

$$\delta E_C = \oint m_{eff} \ddot{u} du. \quad (9)$$

Let an external force F' in the u direction produce a uniform stress σ_u in the u direction within the actuator. Thus the mechanic work done by the external force in one cycle of magnetization is given by:

$$\delta W_{mech} = \oint F' du. \quad (10)$$

The work done by battery during one cycle of the magnetization process is (Venkataraman *et al*., 1998; Venkataraman and Krishnaprasad, 2005):

$$\delta W_{bat} = \nu \oint \mu_0 H dM, \quad (11)$$

where, μ_0 is the permeability of free space.

Consider one cycle of magnetization like external change in $[0;T]$ interval, $H(0) = H(T)$ and $M(0) = M(T)$ then $\oint HdH = \oint MdM = 0$. with this condition, Eq. (11) become:

$$\delta W_{bat} = \nu \oint \mu_0 H dM + \underbrace{\nu \oint \mu_0 \alpha M dM}_{0}. \quad (12)$$

Substituting Eq. (4), (6), (7), (8), (9), (10), (12) in to Eq. (1) we obtain the following equation:

$$\begin{aligned}&\nu\mu_0\oint\left(H+\alpha M-\frac{2bMu}{\mu_0}\right)dM+\\&\oint\left(F'-\nu bM^2-k_1u-k_3u^3-c_l\dot{u}-m_{eff}\ddot{u}\right)du=\delta W_{mag}\\&+\nu\oint k\,sign(\dot{H})(1-c)dM_{irr}.\end{aligned}\tag{13}$$

We define effective field to be:

$$H_{eff}=H+\alpha M-\frac{2bMu}{\mu_0},\tag{14}$$

By integration of the first term of Eq. (13) over one cycle of magnetization, we have:

$$\oint H_{eff}\,dM=-\oint M\,dH_{eff}=0.\tag{15}$$

The magnetic potential energy for the lossless case is given by (Venkataraman *et al*., 1998; Calkins *et al*., 2000):

$$\delta W_{mag}=-\nu\mu_0\oint M_{an}dH_{eff},\tag{16}$$

Thus Eq. (13) can be rewritten as:

$$\begin{aligned}&\nu\mu_0\oint\left(M_{an}-M-\frac{k\,sign(\dot{H})(1-c)}{\mu_0}\frac{dM_{irr}}{dH_{eff}}\right)dH_{eff}+\\&\oint\left(F'-\nu bM^2-k_1u-k_3u^3-c_l\dot{u}-m_{eff}\ddot{u}\right)du=0.\end{aligned}\tag{17}$$

Note that the above equation is valid only if H, M, u and $\dot{u}$ are periodic functions of time. We make the hypothesis that the following equation is valid when we go from one point to another point on this periodic orbit:

$$\begin{aligned}&\nu\mu_0\int\left(M_{an}-M-\frac{k\,sign(\dot{H})(1-c)}{\mu_0}\frac{dM_{irr}}{dH_{eff}}\right)dH_{eff}+\\&\int\left(F'-\nu bM^2-k_1u-k_3u^3-c_l\dot{u}-m_{eff}\ddot{u}\right)du=0.\end{aligned}\tag{18}$$

This equation is assumed to hold only on the periodic orbit. Since du and dH_{eff} are independent variations arising from independent control of external prestress and applied magnetic field respectively, the integrands must be equal to zero:

$$\begin{cases}M_{an}-M-\dfrac{k\,sign(\dot{H})(1-c)}{\mu_0}\dfrac{dM_{irr}}{dH_{eff}}=0\\ m_{eff}\ddot{u}+c_l\dot{u}+k_1u+k_3u^3+\nu bM^2=F'\end{cases}.\tag{19}$$

Jiles and Atherton relate the irreversible and the reversible magnetization as follows (Krzysztof and Szczyglowski, 2007; Xiaojing and Le, 2007):

$$M=M_{rev}+M_{irr},\tag{20}$$

$$M_{rev}=c\left(M_{an}-M_{irr}\right),\tag{21}$$

Thus:

$$\frac{dM}{dH}=\delta_M(1-c)\frac{dM_{irr}}{dH}+c\frac{dM_{an}}{dH},\tag{22}$$

where, δ_M is defined by:

$$\delta_M=\begin{cases}0:\ \mathrm{H}<0\ \text{and}\ \mathrm{M_{an}}(H_{eff})-M(H)>0\\ 0:\ \mathrm{H}>0\ \text{and}\ \mathrm{M_{an}}(H_{eff})-M(H)<0\\ 1\quad\text{otherwise}\end{cases}\tag{23}$$

Finally after some algebraic manipulations, the equations of our model can be obtained as follows:

$$\begin{cases}\dot{\mathrm{M}}=\dfrac{\dfrac{ck\,sign(\dot{H})}{\mu_0}\dfrac{dM_{an}}{dH_{eff}}+\delta_M(M_{an}-M)}{\dfrac{k\,sign(\dot{H})}{\mu_0}-\left[\dfrac{ck\,sign(\dot{H})}{\mu_0}\dfrac{dM_{an}}{dH_{eff}}+\delta_M(M_{an}-M)\right]\left(\alpha-\dfrac{2bu}{\mu_0}\right)}\dot{H},\\ \ddot{u}+2\xi\omega_0\dot{u}+\omega_0^2u+\beta u^3+\dfrac{\omega_0^2l\lambda_s}{M_s^2}M^2=f'\end{cases}\tag{24}$$

where,

$$\begin{aligned}&\omega_0^2=\frac{k_1}{m_{eff}};\ 2\xi\omega_0=\frac{c_l}{m_{eff}};\ \beta=\frac{k_3}{m_{eff}};\\&\frac{\omega_0^2l\lambda_s}{M_s^2}=\frac{b\nu}{m_{eff}};\ f'=\frac{F'}{m_{eff}}\end{aligned}\tag{25}$$

RESULTS AND DISCUSSION

Mechanical part of the model: The material using in this analysis is Terfenol-D rod, for his best magnetostrictive performance. The parameters given by Venkataraman *et al*. (1998), Venkataraman and Krishnaprasad (1999), Dapino *et al*. (1998), Tan and Baras (2004), Jiaju *et al*. (2007),

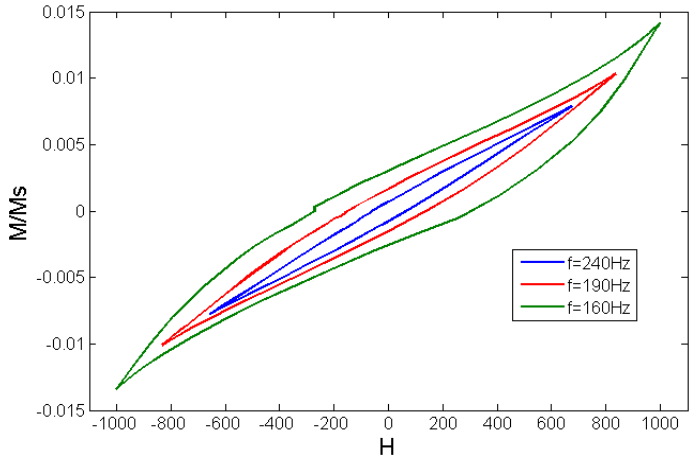

Fig. 2: Magnetic hysteresis loops under different exciting frequency for $\overline{\beta} = 38.57; U_0 = 700kV$

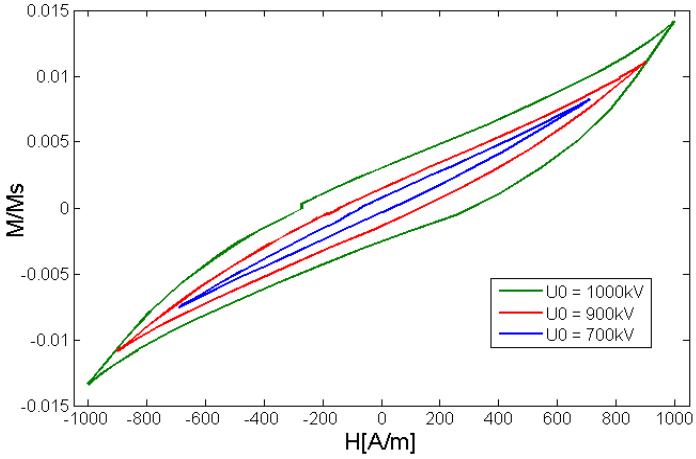

Fig. 3: Magnetic hysteresis loops under different exciting amplitude for $f = 160Hz; \overline{\beta} = 38.57$

Sturos *et al*. (1995) and Willams *et al*. (2006) are: length $(l = 11{,}5cm)$; diameter $(D = 12{,}7mm)$; mass $(m_l = 0{,}5kg)$; damping coefficient $(c_l = 10^3 Ns/m)$; Young's modulus $(E = 30 \times 10^9 Pa)$; magnetostriction coefficient $(\lambda_s = 1000 \times 10^{-6})$:

$$k_1 = 3{,}8 \times 10^6 N/m;\ k_3 = 1{,}25 \times 10^9 N/m^3;$$
$$M_s = 7{,}65 \times 10^5;\ c = 0{,}18;\ k = 40;\ b = 2{,}1;\ \alpha = -0{,}0157;$$
$$\xi = 0{,}3627;\ f^{'} = 0{,}0.$$

Taking periodic excitative external field in the form:

$$\dot{H} = U_0 \cos \omega t, \tag{26}$$

Figure 2 and 3 show that the frequency and amplitude of exciting field have remarkable influence on the magnetic hysteresis loops. Figure 4 on his part shows that, the mechanical nonlinear parameter does not have remarkable influence on the magnetic hysteresis loops. Figure 5, the magnetization take the sinusoidal form with some parameter.

According to Willams *et al*. (2006) and Kalmar-Nagy and Shekhawat (2009) and Fig. 5 the magnetization takes the sinusoidal form with some amplitude and frequency exciting. In that case:

$$M = M_{\max} \sin \omega t. \tag{27}$$

If we suppose that the material is not submitted to any external force $(f^{'} = 0)$, after some manipulation, the mechanical part of the model takes Duffing type equation in form:

$$\ddot{u} + \omega_0^2 u = -2\xi\omega_0 \dot{u} - \beta u^3 - Q_0 \sin^2 \omega t, \tag{28}$$

We non dimensionalise the time scale t by set nondimensional time $\tau = \Omega t$, where Ω is the natural frequency; and order the equation by introducing the small parameter ε.

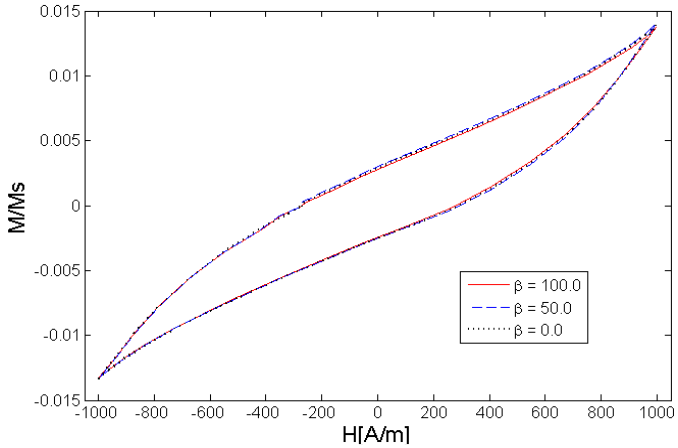

Fig. 4: Mechanical nonlinear effect on the magnetic hysteresis loops for $U_0 = 700kV; f = 160Hz$

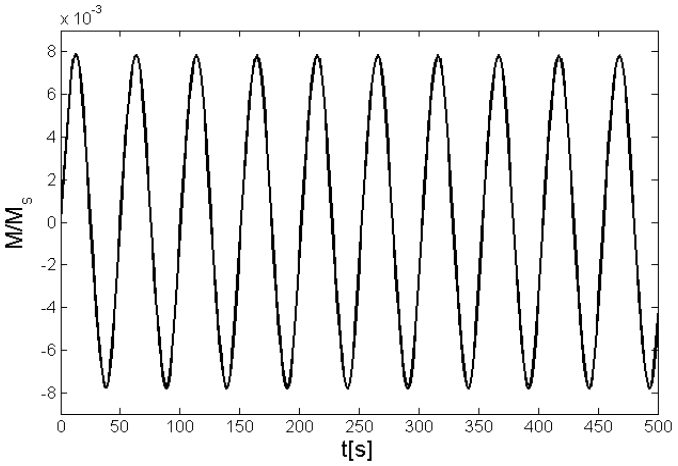

Fig. 5: Magnetization response versus time for $U_0 = 700kV; f = 160Hz; \overline{\beta} = 38.57$

The equation of motion become:

$$u'' + \omega_0^2 u = -2\varepsilon\xi\omega_0 u' - \varepsilon\overline{\beta}u^3 - \varepsilon\overline{Q_0}\sin^2\varpi\tau, \quad (29)$$

where,

$$\varpi_0 = \frac{\omega_0}{\Omega}, \ \overline{\beta} = \frac{\beta}{\Omega^2}, \ \overline{Q_0} = \frac{Q_0}{\Omega^2}, \text{ and } \varpi = \frac{\omega}{\Omega}.$$

Approximate solution: An approximate solution is generally obtained as follows (Chengying and Jin, 2010; Lévine, 2004; Nayfeh and Mook, 1979):

$$u(\tau,\varepsilon) = u_0(T_0,T_1) + \varepsilon u_1(T_0,T_1) + \ldots \quad (30)$$

where, $u(T_0,T_1)$ are functions of time scale T_n for $n = 0,1,\ldots$ yet to be determined and ε is arbitrarily small parameter. The derivative perturbations rely on the notion that the real time τ, can be expressed in the form of set of successively independent time scales, T_n given by:

$$T_n = \varepsilon^n \tau \quad n = 0,1,\ldots \quad (31)$$

In Eq. (30) T_0 is nominally considered as a fast time-scale and T_1 as slower time scale, such that $T_0 = \tau$, $T_1 = \varepsilon\tau$ as from Eq. (31). It follows that the derivatives with respect to τ become expansions in terms of the partial derivatives with respect to the T_n according to:

$$\frac{d}{d\tau} = D_0 + \varepsilon D_1 + \ldots \quad (32)$$

$$\frac{d^2}{d\tau^2} = D_0^2 + 2\varepsilon D_0 D_1 + \ldots \quad (33)$$

Substituting Eq. (30), (32), (33) into Eq. (29) and collecting the coefficients of like order of ε^n, and equating them to zero in order to construct the perturbation equations, leads to:

- Ordre ε^0 :

$$D_0^2 u_0 + \varpi_0^2 u_0 = 0. \quad (34)$$

- Ordre ε^0 :

$$D_0^2 u_1 + \varpi_0^2 u_1 = -2D_0 D_1 u_0 - 2\xi\varpi_0 D_0 u_0 - \overline{\beta} u_0^3 - \overline{Q}_0 \sin^2 \varpi\tau. \quad (35)$$

Harmonic solution of the zeroth order perturbation is:

$$u_0(T_0, T_1) = A(T_1)e^{j\varpi_0 T_0} + \overline{A}(T_1)e^{-j\varpi_0 T_0}, \quad (36)$$

Substitutingzeroth order perturbation solution into the first order perturbation give:

$$D_0^2 u_1 + \varpi_0^2 u_1 = \left(-2j\varpi_0 \frac{dA}{dT_1} - 2j\xi\varpi_0^2 A - 3\overline{\beta}A^2\overline{A}\right) e^{j\varpi_0 T_0} - \overline{\beta}A^3 e^{3j\varpi_0 T_0} + \frac{\overline{Q}_0}{4}e^{2j\varpi_0 T_0} + Cc + \frac{\overline{Q}_0}{2}, \quad (37)$$

To include near-resonant terms within the secular term, a detuning parameter σ is introduced by:

$$2\varpi = \varpi_0 + \varepsilon\sigma. \quad (38)$$

The secular condition become:

$$-2j\varpi_0 \frac{dA}{dT_1} - 2j\xi\varpi_0^2 A - 3\overline{\beta}A^2\overline{A} + \frac{\overline{Q}_0}{4}e^{j\sigma T_1} = 0. \quad (39)$$

In Eq. (39) the complex amplitude A can be expressed in polar form:

$$A = \frac{a}{2}e^{j\varphi}, \quad (40)$$

Substituting Eq. (40) in to Eq. (39) and then separating out the real and imaginairy parts of the resulting equation, we obtained:

$$\begin{cases} \varpi_0 \dfrac{da}{dT_1} = -\xi\varpi_0^2 a + \dfrac{\overline{Q}_0}{4}\sin\gamma \\ \varpi_0 a \dfrac{d\gamma}{dT_1} = \varpi_0 a\sigma - \dfrac{3}{8}\overline{\beta}a^3 + \dfrac{\overline{Q}_0}{4}\cos\gamma \end{cases}, \quad (41)$$

where,

$$\gamma = \sigma T_1 - \varphi.$$

For steady-state conditions, the slowly varying amplitude and phase are set to zero $(\frac{da}{dT_1} = \frac{d\gamma}{dT_1} = 0)$. Then Eq. (41) become:

$$a^2\varpi_0^2\left[\xi^2\varpi_0^2 + (\sigma - \frac{3}{8\varpi_0}\overline{\beta}a^2)^2\right] - \frac{\overline{Q}_0^2}{16} = 0. \quad (42)$$

Which give the amplitude of response a as function of the detuning parameter σ.

Different parameters effect to system response: Figure 6 to 8 show that nonlinear parameter, amplitude force and damping parameter affect the amplitude response of the system.

Figure 9 shows that, with some value of detuning parameter σ the amplitude response is simple and for other the amplitude response is multiple.

Stability analysis for vibration system: Let us take Eq. (41) in the follows:

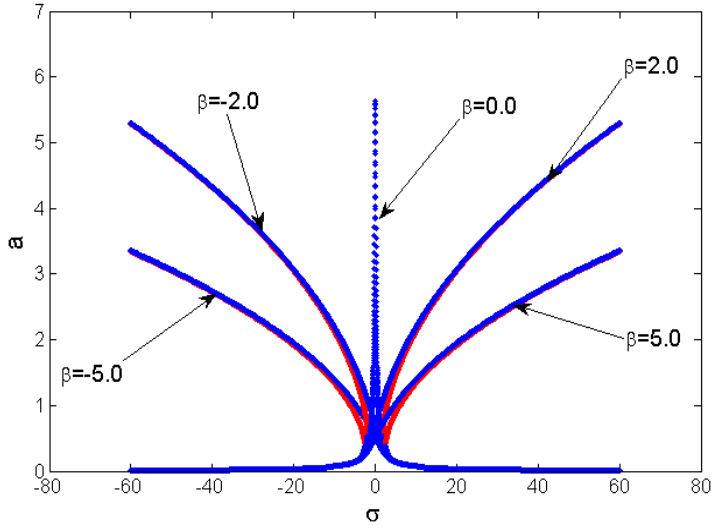

Fig. 6: Nonlinear effect on the system response for $\varpi_0 = 0.35; \xi = 0.3627; \overline{Q}_0 = 1$

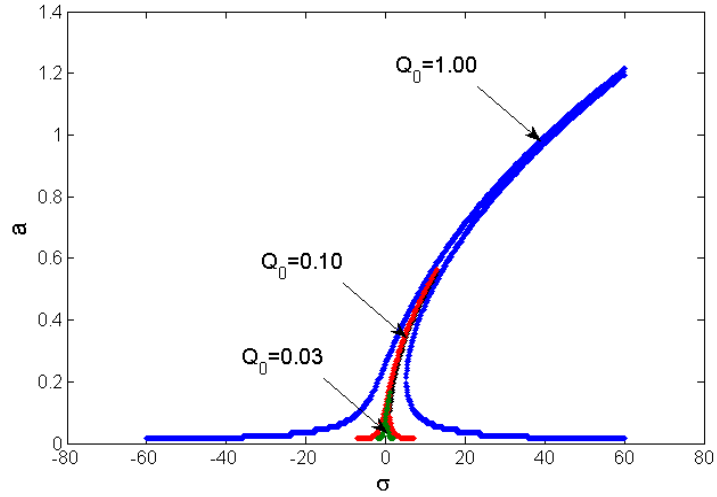

Fig. 7: Amplitude force effect to system response for $\varpi_0 = 0.35; \xi = 0.3627; \overline{\beta} = 38.57$

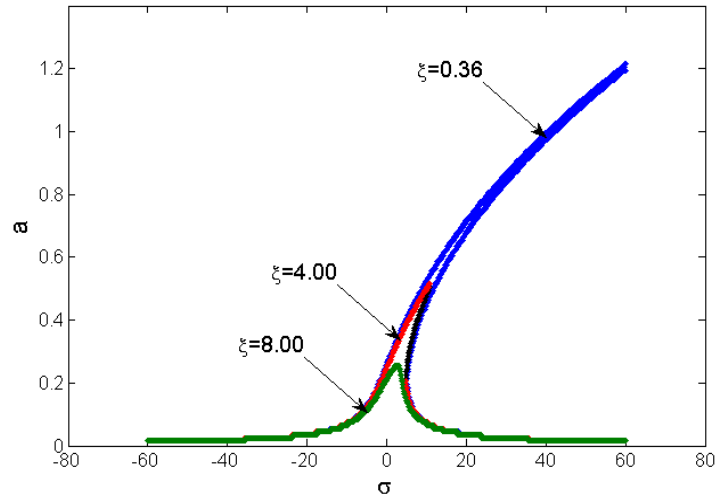

Fig. 8: Damping coefficient effect to system response for $\varpi_0 = 0.35; \overline{\beta} = 38.57; \overline{Q}_0 = 1$

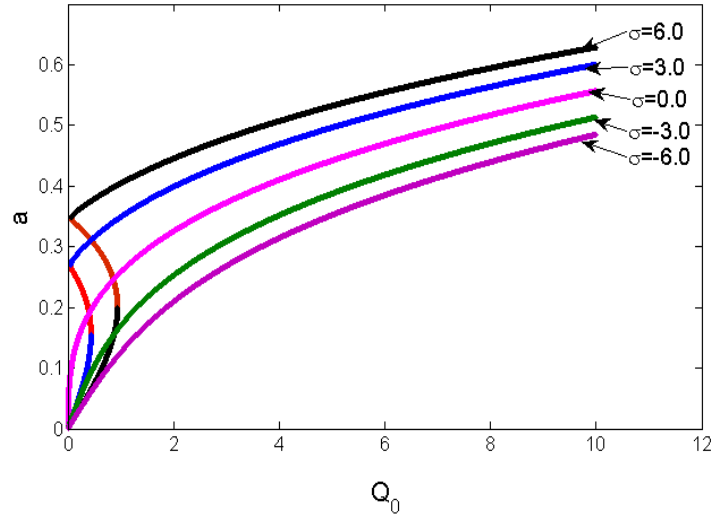

Fig. 9: Amplitude response versus the amplitude of excitative force for $\varpi_0 = 0.35; \xi = 0.3627; \overline{\beta} = 38.57$

$$\begin{cases} -\varpi_0 \dfrac{da}{dT_1} - \xi \varpi_0^2 a + \dfrac{\overline{Q}_0}{4}\sin(\sigma T_1 - \varphi) = 0 \\ \varpi_0 a \dfrac{d\varphi}{dT_1} - \dfrac{3}{8}\overline{\beta} a^3 + \dfrac{\overline{Q}_0}{4}\cos(\sigma T_1 - \varphi) = 0 \end{cases}. \tag{43}$$

The solution of Eq. (41) is given in the following form:

$$\begin{aligned} a &= a_0 + \delta a \\ \varphi &= \gamma_0 + \delta\gamma \end{aligned} \tag{44}$$

Eq. (44) in Eq. (43) gives:

$$\begin{cases} (a_0' + \delta a') = -\xi \varpi_0 (a_0 + \delta a) + \dfrac{\overline{Q}_0}{4\varpi_0}\sin(\gamma_0 + \delta\gamma) \\ (a_0 + \delta a)(\gamma_0' + \delta\gamma') = \sigma(a_0 + \delta a) - \dfrac{3}{8\varpi_0}\overline{\beta}(a_0 + \delta a)^3 + \dfrac{\overline{Q}_0}{4\varpi_0}\cos(\gamma_0 + \delta\gamma) \end{cases}, \tag{45}$$

The transformation of Eq. (45) in sin and cos terms with the fact that $\sin\delta\gamma \to \delta\gamma$ and $\cos\delta\gamma \to 1$ and consider only the linear terms in δa and $\delta\gamma$, Eq. (45) becomes:

$$\begin{cases} a_0' + \xi\varpi_0 a_0 - \dfrac{\overline{Q}_0}{4\varpi_0}\sin\gamma_0 = -\delta a' - \xi\varpi_0\delta a + \dfrac{\overline{Q}_0}{4\varpi_0}\delta\gamma\cos\gamma_0 \\ a_0\gamma_0' - \sigma a_0 + \dfrac{3}{8\varpi_0}\overline{\beta}a_0^3 - \dfrac{\overline{Q}_0}{4\varpi_0}\sin\gamma_0 = -a_0\delta\gamma' + \sigma\delta a - \dfrac{9}{8\varpi_0}\overline{\beta}a_0^2\delta a - \dfrac{\overline{Q}_0}{4\varpi_0}\delta\gamma\sin\gamma_0 \end{cases}. \tag{46}$$

The left hand side of Eq. (46) is equal to zero at the equilibrium point. Eq. (46) becomes:

$$\begin{cases} -\delta a' - \xi\varpi_0\delta a + \dfrac{\overline{Q}_0}{4\varpi_0}\delta\gamma\cos\gamma_0 = 0 \\ -a_0\delta\gamma' + \sigma\delta a - \dfrac{9}{8\varpi_0}\overline{\beta}a_0^2\delta a - \dfrac{\overline{Q}_0}{4\varpi_0}\delta\gamma\sin\gamma = 0 \end{cases}. \tag{47}$$

The solution of Eq. (47) is follows as:

$$\begin{aligned} \delta a &= \delta a^* e^{\lambda T_1} \\ \delta\gamma &= \delta\gamma^* e^{\lambda T_1} \end{aligned} \tag{48}$$

where, δa^* and $\delta\gamma^*$ are small perturbation of amplitude and phase respectively.
Eq. (48) in Eq. (47) give Eq. (49) in the follows form:

$$\begin{bmatrix} -(\lambda + \xi\overline{\varpi}_0) & -a_0(\sigma - \dfrac{3}{8\varpi_0}\overline{\beta}_0^2) \\ \dfrac{1}{a_0}(\sigma - \dfrac{9}{8\varpi_0}\overline{\beta}_0^2) & -(\lambda + \xi\varpi_0) \end{bmatrix} \begin{bmatrix} \delta a^* \\ \delta\gamma^* \end{bmatrix} = \begin{bmatrix} 0 \\ 0 \end{bmatrix}, \tag{49}$$

where, the stability matrix is given as the follows expression:

$$M = \begin{bmatrix} -(\lambda + \xi\overline{\varpi}_0) & -a_0(\sigma - \dfrac{3}{8\varpi_0}\overline{\beta}_0^2) \\ \dfrac{1}{a_0}(\sigma - \dfrac{9}{8\varpi_0}\overline{\beta}_0^2) & -(\lambda + \xi\varpi_0) \end{bmatrix}. \tag{50}$$

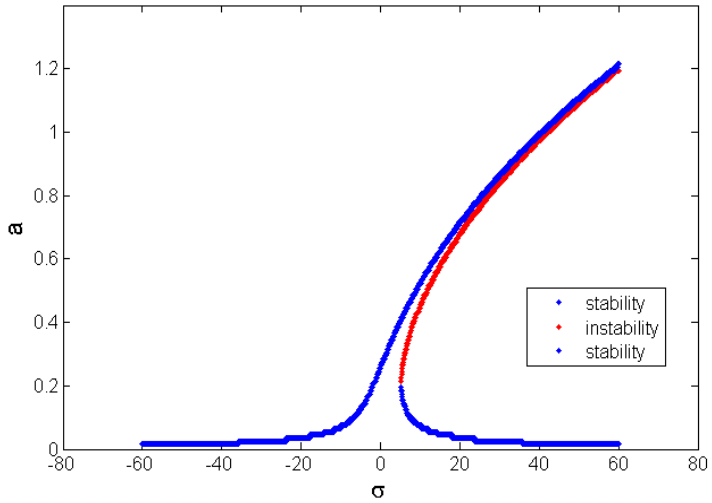

Fig. 10: Variation of the amplitude of the response according to the parameter of perturbation for $\varpi_0 = 0.35; \xi = 0.3627; \overline{\beta} = 38.57; \overline{Q}_0 = 1$

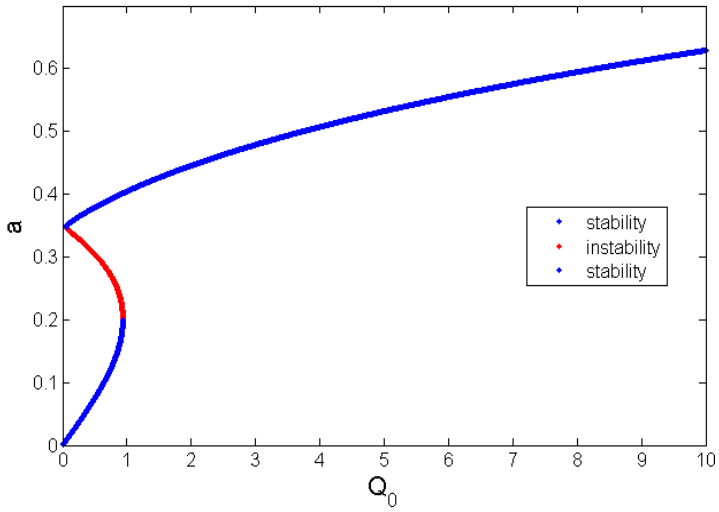

Fig. 11: Variation of the amplitude of the response according to the amplitude of the excitation force for $\varpi_0 = 0.35; \xi = 0.3627; \overline{\beta} = 38.57; \overline{Q}_0 = 4$

The characteristic equation of Eq. (50) is follows as:

$$\lambda^2 + 2\xi\varpi_0\lambda + \xi^2\varpi_0^2 + (\sigma - \frac{9}{8\varpi_0}\overline{\beta}a_0^2)$$
$$(\sigma - \frac{3}{8\varpi_0}\overline{\beta}a_0^2) = 0 \quad (51)$$

According to the stability criterion of Routh-Hurwitz (Lacheisserie and Cyrot, 2000; Lakshmanan and Rajaseekar, 2003), the characteristic equation must have real solutions or with negative real parts. What stipulates that:

$$\xi^2\varpi_0^2 + (\sigma - \frac{9}{8\varpi_0}\overline{\beta}a_0^2)(\sigma - \frac{3}{8\varpi_0}\overline{\beta}a_0^2) \succ 0 \quad (52)$$

Figure 10 and 11, we have the domain of stability in blue and field of instability in red.

Bifurcation and chaotic analysis for vibration system: Let us take Eq. (28) in form:

$$\begin{cases} u_1' = u_2 \\ u_2' = -2\xi\varpi_0 u_2 - \varpi_0^2 u_1 - \overline{\beta}u_1^3 - \overline{Q_0}\sin^2\varpi\tau \end{cases} \quad (53)$$

System (53) is solved numerically to define routes to chaos in our model using the standard fourth-order Runge-Kutta algorithm. For the set of parameters used in this work, the time step is always $\Delta t \le 0.005$ and computations are performed using variables and constants parameters in extended mode. For each parameters combination, the system is integrated for

sufficiently long time and transient is discarded. Two indicators are used to identify the type of transition leading to chaos (Lévine, 2004; Mabekou, 2008; Zeng *et al*., 2008). The first indicator is the bifurcation diagram and the second is the largest one dimensional (1D) numerical Lyapunov exponent defined by:

$$\lambda_{\max} = \lim_{t\to\infty}\left[\frac{1}{t}\ln(d(t))\right], \tag{54}$$

where,

$$d(t) = \sqrt{\delta_1^2 + \delta_2^2}. \tag{55}$$

And computed from following variational equation obtained by perturbing the solutions of Eq. (53) as follows: $u_1 \to u_1 + \delta_1$ and $u_2 \to u_2 + \delta_2$ is the distance between neighbouring trajectories; asymptotically $\delta(t) = \exp(\lambda_{\max} t)$. Thus, if $\lambda_{\max} \succ 0$, neighbouring trajectories diverge and the state of the system is chaotic. For $\lambda_{\max} \prec 0$, these trajectories converge and the state of the system is non-chaotic. The case $\lambda_{\max} = 0$, corresponds to the torus state of the system.

We now focus on the effects of biasing on the dynamics of the system modelled by Eq. (53). To achieve this goal, $\bar{Q}_0$ is chosen as control parameter and the rest of system parameters are assigned the following values:

$$\varpi_0 = 0.35; \quad \xi = 0.3627; \quad \bar{\beta} = 38.57; \quad \omega = 1$$

Figure 12 shows the bifurcation diagram and the corresponding lyapounov function. Therefore the scanning process is performed to investigate the sensitivity of the system to tiny change in $\bar{Q}_0$. The range $0.00 \le \bar{Q}_0 \le 100$ is considered to monitor the bifurcation control parameter. It is found that the system can exhibit complex dynamic motions including periodic, multiperiodic and chaos states. Indeed, for the values of system parameters defined above, various scemarios/routes to chaos are observed such as period doubling and crisis scemarios to chaos. Sample results are provided in Fig. 13 where we show a bifurcation diagram associated with the corresponding graph of largest 1D numerical lyapunov exponent. This bifurcation diagram is obtained by plotting the displacement in the material in terms of the control parameter $\bar{Q}_0$ whereas the lyapunov exponent graph is obtained by simultaneously integrating Eq. (53) and Eq. (54) -Eq. (55). The positive value of λ_{max} is signature of chaotic behaviour. Figure 14 shows the Poincare section. Figure 13 shows a sample result of the scenario

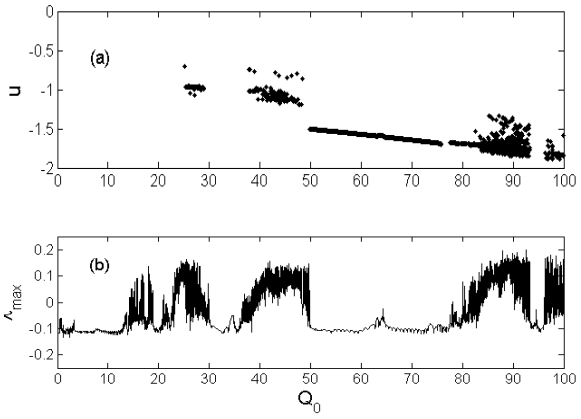

Fig. 12: Bifurcation diagram of the system (a) and the graph of 1D largest Lyapunov exponent (b) for $\varpi_0 = 0.35; \xi = 0.3627; \bar{\beta} = 38.57$

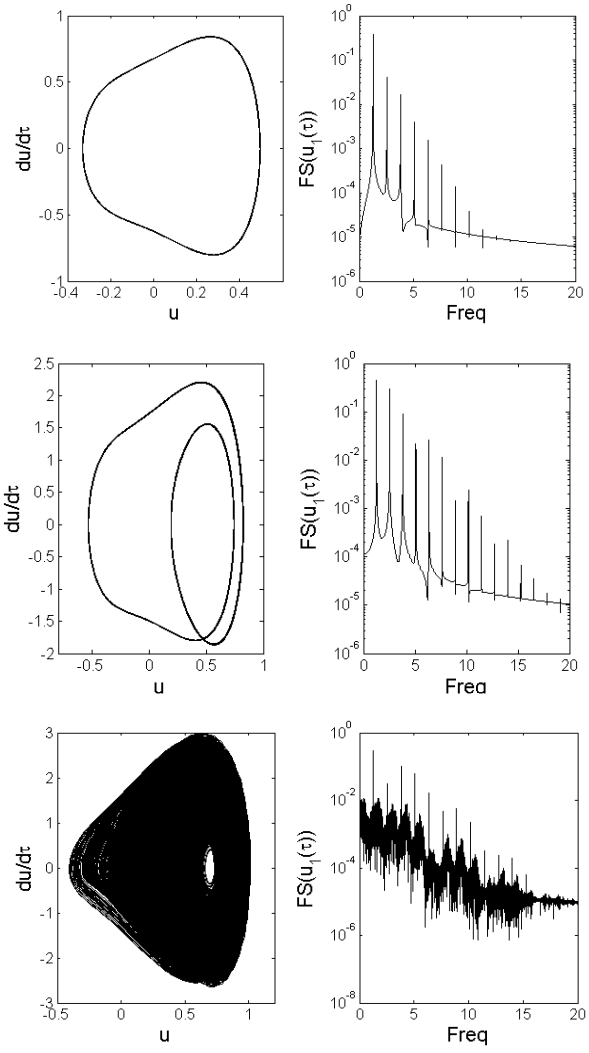

Fig. 13: Numerical phase portraits of the system (left) and the corresponding FS spectra (right). (a) period-1 for $\bar{Q}_0 = 1$, (b) period-2 for $\bar{Q}_0 = 7$ (c), Chaotic attractor for $\bar{Q}_0 = 14$

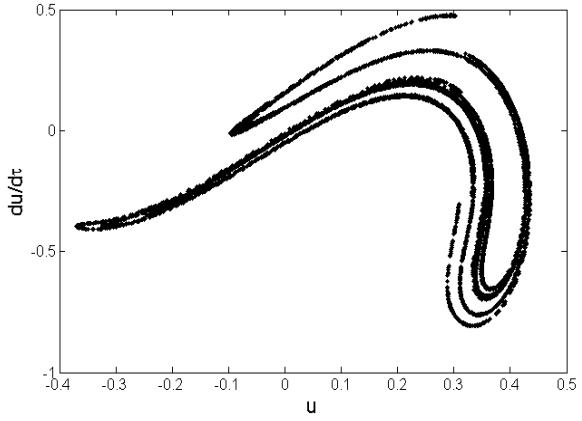

Fig. 14: Poincare section for for $\varpi_0 = 0.35; \xi = 0.3627;$ $\overline{\beta} = 38.57; \overline{Q}_0 = 14$

to chaos. We observed it by plotting phase portraits with their corresponding power spectrum.

CONCLUSION

In this study we have used the energy principle balance to obtain the equation of model by taking into account the nonlinear effect of material. The mathematical model of the material is presented. Using the multiple time scale method, the approximate solution of our model is obtained. The numerical results present the effect of the nonlinearity of the material, damping and the amplitude of the magnetic force on the stability and chaotic response of the system. In the future work we aim to extend the nonlinearity order five and consider the eddy current, temperature and external force effect.

REFERENCES

Calkins, F.T., R.C. Smith and A.B. Flatau, 2000. An energy-based hysteresis model for magnetostrictive transducers. IEEE T. Magn., 36(2): 429-439.

Chengying, L. and Z. Jin, 2010. An analysis of a magnetostrictive actuator in nonlinear dynamic. Proceeding of the International Conference on Information, Electronic and Computer Science, pp: 1381-1387.

Dapino, M.J., R.C. Simith and A.B. Flatau, 1998. Active and structural strain model for magnetostrictive transducers. Proceeding of the 5th Annual International Symposium on Smart Structures and Materials, pp: 198-209.

Jiaju, Z., C. Shuying, W. Hongli and H. Wenmei, 2007. Hybrid genetic algorithms for parameter identification of a hysteresis model of magnetostrictive actuators. Neurocomputing, 70: 749-761.

Kalmar-Nagy, T. and A. Shekhawat, 2009. Nonlinear dynamics of oscillator with bilinear hysteresis and sinusoidal excitation. Physica D, 238(17): 1768-1786.

Krzysztof, C. and J. Szczyglowski, 2007. An alternative method to estimate the parameters of Jiles-Atherton model. J. Magn. Magn. Mater., 314: 47-51.

Lacheisserie, E.T. and M. Cyrot, 2000. Magnétisme. II, Matériaux et applications. EDP Sciences, Les Ulis pp: 318-319.

Lakshmanan, M. and S. Rajaseekar, 2003. Nonlinear Dynamics: Integrability, Chaos, and Patterns. Springer-Verlag, Berlin, Heidelberg, pp: 620.

Lévine, J., 2004. Analyse et commande des systèmes non linéaires. Centre Automatique et Systèmes, Ecole des Mines de Paris, pp: 33-77.

Mabekou, T.J.S., 2008. Dynamique des oscillations non-linéaires de la plante sous l'action du vent. M.A. Thèse, Université de Dschang.

Nayfeh, A.H. and D.T. Mook, 1979. Nonlinear Oscillations. Wiley-Interscience, New York, pp: 161-173.

Pérignon, F., 2004. Vibrations forcées des structures minces, élastiques, non linéaires. Ph.D. Thèse, Université Aix-Marseille II, pp: 7-37.

Sturos, T.J., J.W. Sutherland, K.S. Moon, D. Liu and A.R. Kashani, 1995. Application of an actively controlled magnetostrictive actuator to vibration abatement in the turning process. Proc. ASME Dynam. Syst. Control Division (DSC), 57(1): 539-543.

Tan, X. and J.S. Baras, 2002. A robust control framework for smart actuators. Technical Report of the Institute for Systems Research, University of Maryland at College Park.

Tan, X. and J.S. Baras, 2004. Modeling and control of hysteresis in magnetostrictive actuators. Automatica, 40: 1469-1480.

Vankataraman, I.R. and S. Manservisi, 2006. On a low-dimensional model for magnetostriction. Physica B, 372: 378-382.

Venkataraman, I.R. and P.S. Krishnaprasad, 1999. A model for a thin magnetostrictive actuator. Technical Report of the Institute for Systems Research, University of Maryland at College Park.

Venkataraman, I.R. and P.S. Krishnaprasad, 2005. On a low-dimensional model for ferromagnetism. Nonlinear Anal., 61: 1447-1482.

Venkataraman, I.R., J. Rameau and P.S. Krishnaprasad, 1998. Characterization of an extrema MP 50/6 magnetostrictive actuator. Technical Report of the Institute for systems Research, University of Maryland at College Park.

Wang, T.Z. and Y.H. Zhou, 2010. A nonlinear transient constitutive model with eddy current effects for giant magnetostrictive materials. J. Appl. Phys., 108(12): 123905.

Willams, M.C., R.S. Vogelsong and K.S. Kundert, 2006. Simulation and modeling of nonlinear magnetics. Proceeding of the IEEE International Symposium on Circuits and Systems (ISCAS '95), pp: 736-739.

Xiaojing, Z. and S. Le, 2007. A one-dimension coupled hysteresis model for giant magnetostrictive material. J. Magn. Magn. Mater., 309: 263-271.

Zeng, H., C. Chen and D. Pan, 2008. Bifurcation and chaos of giant magnetostrictive actuators. Proc. CSEE, 28(9): 111-115.